Singularities of energy states of localized electrons in strongly compensated n-InSb

V. V. Arendarchuk, E. M. Gershenzon, L. B. Litvak-Gorskaya, and R. I. Rabinovich

Moscow State Pedagogical Institute
(Submitted June 25, 1973)
Zh. Eksp. Teor. Fiz. 65, 2387–2398 (December 1973)

To investigate the energy states of localized electrons in weakly-doped ($N_d a^3 \ll 1$) and strongly compensated ($1 - K \ll 1$) n-InSb, we investigated the dependence of the microwave power absorption coefficient α on the wavelength λ (N_d is the donor density, a is the Bohr radius of the electron on the donor, and K is the degree of compensation). For samples with $K \sim 0.9$ at $T = 1.6 - 4.2°K$ in the energy range $\hbar\omega = 0.2$ to 3.3 Ry (Ry is the ionization energy of the isolated donor and equals 0.67 meV), we observed a number of absorption maxima (peaks). These results can be explained by assuming that the energy spectrum of the localized electrons is analogous to the spectrum of the molecular hydrogen ion H_2^+ with a distance $\sim 1.2 - 3.5$ a between the "nuclei" (donors). In samples with $K \gtrsim 0.99$, the $\alpha(\lambda)$ dependence turns out to be significantly different and cannot be explained by the existing theories.

1. INTRODUCTION

Considerable interest has recently been evinced in the study of the mechanisms of impurity conductivity of weakly doped ($N_d a^3 \ll 1$) and strongly compensated ($1 - K \ll 1$) semiconductors (here N_d is the concentration of the principal impurity – the donors, a is the Bohr radius of the electron at the donor, and K is the degree of compensation). This is explained in part by the possible analogy between the character of the conductivity of such semiconductors and that of the disordered systems[1].

The theory of the static conductivity σ_0 of strongly compensated semiconductors was developed in recent papers by Shklovskiĭ and Éfros[2]. According to them, in semiconductors at $N_d a^3 \ll 1$ and $1 - K \ll 1$, owing to the inhomogeneity in the distribution of the impurities, two types of impurity-potential fluctuations are important, large-scale and small-scale. Among the latter at low temperatures ($T \to 0$), the most important are the potential wells that occur when two charged impurities approach each other and the distance between them becomes

$$R \leqslant R_m \equiv \left[\frac{3}{2\pi}(1-K)\right]^{1/3} N_d^{-1/3} < N_d^{-1/3},$$

i.e., when "impurity pairs" are produced. It is precisely in these wells that most electrons are located at $T \to 0$.

Shklovskiĭ and Éfros[1] investigated the influence exerted on σ_0 only for "classical pairs," i.e., pairs with $R \gg a$. It should be noted that at $R \gg a$ an electron localized on a pair has a near-hydrogen-like energy-level spectrum. We have previously advanced the hypothesis[2] that pairs with $R \sim a$ can be regarded as the analog of a molecular hydrogen ion H_2^+[3] with a characteristic distance $\sim R$ between "nuclei." It is important that the spectrum of the energy levels of H_2^+ differs noticeably at $R \sim a$ from the hydrogen-like levels of the "isolated" donor. The present paper is a continuation and development of[2] and is also devoted to a study of the energy states of localized electrons in n-InSb at $N_d a^3 \ll 1$ and $1 - K \ll 1$. Just as in[2], we investigate here the dependence of the microwave power absorption coefficient α on the wavelength λ of the electromagnetic radiation, but in a much larger frequency interval ($0.2 \text{ Ry} < \hbar\omega < 3.3$ Ry, where Ry is the ionization energy of the isolated donor, equal to 0.67 meV) and in a wider range of values of N_d and K. In addition, we investigate the temperature dependence of the resistivity $\sigma_0^{-1}(T)$.

We note that the high-frequency conductivity (σ_ω) of semiconductors with $N_d a^3 \ll 1$ has been investigated so far theoretically[4] and experimentally (e.g.,[5]) only for the case of low compensation, $K < 0.5$, and in the frequency region $\hbar\omega < 0.2$ Ry[5]. It appears that there is no universally accepted theory of microwave absorption for disordered semiconductors[6].

2. EXPERIMENTAL RESULTS

1. We investigated the dependence of the absorption coefficient on the wavelength $\alpha(\lambda)$ in the range $\lambda = 0.5 - 8.4$ mm ($T = 4.2 - 1.6$ °K) and that of the resistivity $\rho = \sigma_0^{-1}$ on the temperature at $T = 77 - 1$ °K in strongly compensated n-InSb with $N_d \sim 10^{14}$ cm^{-3}. The measurements were performed on samples cut out from one and the same ingot, since the peculiarities of the distribution of the donor and acceptor impurities in InSb make it possible to obtain sets of samples with practically constant donor concentration N_d, but with essentially varying compensation K[7]. To determine N_d and K we used plots of the distribution of Te (residual donor) and Ge (compensating impurity) in InSb by the procedure described earlier[7]. The parameters of the investigated samples are listed in Table I (N_a is the acceptor concentration). To describe the character of the relative variation of N_d and of K from sample to sample, the absolute values of N_d and K are given with exaggerated accuracy.

The values of $\alpha(\lambda)$ were measured on plates with dimensions $7.2 \times 3.4 \times 1 - 0.5$ mm, while the $\rho(T)$ were measured on dumbbells with dimensions (without the lateral probes) $8 \times 1 \times 1$ mm, cut in the immediate vicinity of the plates. All the samples were polished and etched in CP-4A.

TABLE I. Parameters of samples

Sample No.	N_d, cm^{-3}	$N_d - N_a$*, cm^{-3}	K	Activation energy, meV	
				ε_1	ε_3
1	$1.2 \cdot 10^{14}$	$1.8 \cdot 10^{13}$	0.85	1.0	0.3
2	$1.2 \cdot 10^{14}$	$1.3 \cdot 10^{13}$	0.89	1.5	0.8
3	$1.3 \cdot 10^{14}$	$8 \cdot 10^{12}$	0.94	2.0	1.0
4	$1.4 \cdot 10^{14}$	$1 \cdot 10^{12}$	0.99	—	—
5	$1.4 \cdot 10^{14}$	$1 \cdot 10^{11}$	0.99	—	—
6	$1.5 \cdot 10^{14}$	10^{11}	0.99	—	—

*N_a–acceptor concentration.

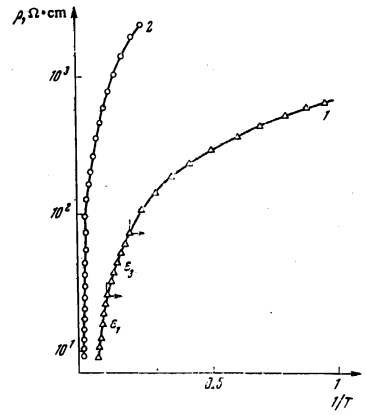

FIG. 1. Temperature dependence of the resistivity at T = 77 – 1°K. 1–Sample No. 3; 2–sample No. 6. The arrows indicate the limits of the section.

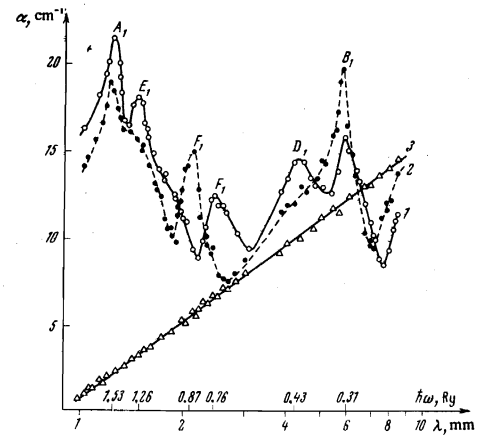

FIG. 2. Dependence of the absorption coefficient α on the wavelength λ for sample No. 1: 1–T = 4.2°K, E = 0; 2–T = 1.6°K, E = 0; 3–T = 4.2°K, E > E_{imp}. The peaks are marked by Latin letters.

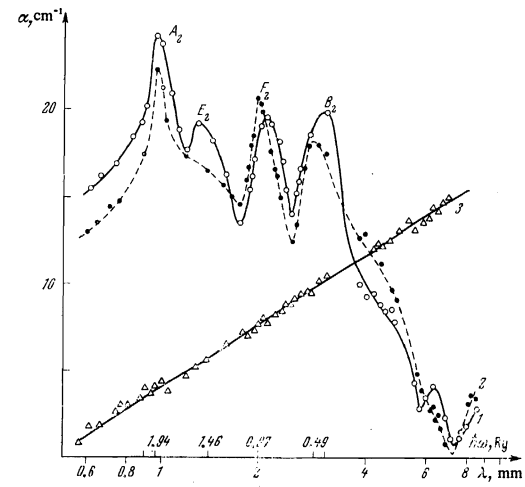

FIG. 3. Dependence of the absorption coefficient α on the wavelength λ in sample No. 2. The notation is the same as in Fig. 2.

We used a standard procedure for the measurement of ρ(T). The distinguishing features of the determination of α(λ) are described in detail in[8] (for the wavelength band 3.8–8.4 mm). The measurements were based on the fact that n-InSb cooled to T ≲ 4.2°K is a sensitive receiver of millimeter and submillimeter radiation[9]. If the sample and receiver are made from identical material with identical values of N_d and K (and consequently with identical dependences σ(E) of the electric conductivity on the electric field intensity), then we can measure the absorption in the n-InSb sample by placing the sample and the receiver in a waveguide (λ ≳ 2 mm) or in a quasioptical channel (λ < 2 mm) one directly after the other.

For the measurement of α(λ) we used backward-wave tubes[10] in the band λ = 0.5–3 mm and klystron generators in the band λ = 3.8–8.4 mm. In order for the background radiation from the warm part of the cryostat not to strike the sample, we used filters of cooled crystalline quartz. In the quasioptical channel, provision was made for illumination of the sample with an incandescent lamp.

2. To determine the character of the impurity conductivity we investigated the temperature dependence of the resistivity, ρ(T). By way of example, Fig. 1 shows plots of ρ(T) of samples No. 3 and No. 6 at T = 1–77°K, inasmuch as the character of the ρ(T) dependence for less compensated samples (Nos. 1–3) was the same and differed significantly from ρ(T) for the more compensated samples (Nos. 4–6). We note that the distance along the crystal-growth axis between samples No. 1 and No. 3 and between No. 4 and No. 6 was 3–5 mm; the distance between samples No. 3 and No. 4 was ~10 mm.

Samples 1–3 are characterized by the presence of sections in which ρ(T) has an exponential dependence. Measurements in magnetic fields[11] and comparison with theory[1] have shown that the low-temperature exponential section corresponds to hopping impurity conductivity with activation energy ϵ_3, and that the high-temperature exponential section corresponds to the activation energy ϵ_1 of the band conductivity. The values of ϵ_1 and ϵ_3 are given in Table I. We see that ϵ_1 exceeds the ionization energy of the isolated donor by a factor 1.5–2.5.

In samples 4–6 there are no sections where ρ(T) is exponential. It can be assumed that their energies ϵ_1 and ϵ_3 are so large that the intrinsic conductivity has already become manifest in the corresponding temperature interval. Such a situation, as applied to p-InSb, was discussed by us earlier[7]. As T → 0, all the samples exhibit hopping conductivity with an activation energy that decreases with decreasing temperature[1], where $\rho(T) \propto \exp(T_0/T)^{1/4}$.

3. Figures 2–4 show plots of the α(λ) of samples 1–3 at 4.2 and 1.6°K in the absence of a constant electric field on the sample (E = 0, curves 1 and 2) and in a field E exceeding by several times the impurity-breakdown field E_{imp}[12] (curves 3), i.e., for localized and free electrons, respectively. We see that for free electrons α decreases monotonically with decreasing λ, and that for localized electrons there are maxima (peaks) of absorption on the α(λ) plot. With increasing compensation, the short-wave absorption peak shifts towards smaller λ; thus it corresponds to 1.05 meV (1.53 Ry) and 1.75 meV (2.6 Ry) for samples 1 and 3, respectively. (See Figs. 2–4). We note that the energy corresponding to the short-wave absorption peak is close to ϵ_1 (see Table I). In addition, longer-wavelength absorption peaks are also observed. All peaks become narrower with decreasing temperature, and shift towards shorter wavelengths. Some of the peaks vanish with decreasing temperature. We note that this was not observed earlier[2] when the background radiation was not filtered out.

Figure 5 illustrates the influence of "band-band" illumination on the character of α(λ) for sample No. 3. We see that illumination makes the shortwave absorption

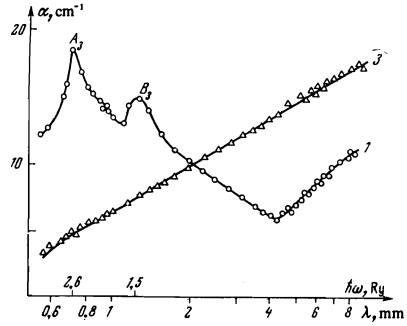

FIG. 4. Dependence of the absorption coefficient α on the wavelength λ in sample No. 3. The notation is the same as in Fig. 2.

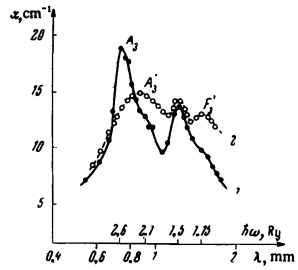

FIG. 5. Influence of "band-band" illumination on the α(λ) dependence in sample No. 3: 1—α(λ) in the absence of illumination; 2—α(λ) when the sample is illuminated with an incandescent lamp.

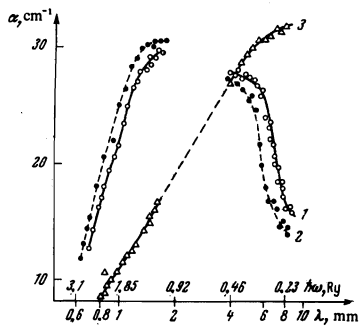

FIG. 6. Dependence of α(λ) of sample No. 5. The notation is the same as in Fig. 2.

peak more smeared out and shifts it towards longer wavelengths, from λ = 760μ to λ = 900μ.

For the more strongly compensated samples Nos. 4–6, the plots of α(λ) are similar to each other, but they are substantially different from those of Figs. 2–4. Let us consider sample No. 5 by way of example (see Fig. 6). The plot of α(λ) is bell-shaped, and lowering the temperature leads to a shift of the entire curve towards shorter wavelengths with practically no change in its shape and integral absorption. When a strong electric field is applied, α(λ) decreases monotonically with decreasing λ.

We note that, just as in[13], the maximum value α_m of α(λ) for all samples, unlike the case of almost free electrons, greatly exceeds the value $\alpha_0 = 4\pi\sigma_0/c\kappa^{1/2}$ corresponding to the static conductivity (κ is the dielectric constant). Thus, for example, $\alpha_m/\alpha_0 = 12$ for sample No. 1 and $\approx 6 \times 10^2$ for sample No. 6 at 4.2°K.

It follows from the foregoing experimental results that the absorption spectrum in strongly compensated n-InSb differs noticeably from hydrogenlike. The presence of absorption peaks for samples Nos. 1 and 3 allows us to assume that the absorption is due to the transitions of the electrons between the localized states.

3. THE H_2^+ MODEL

The previously proposed[2] H_2^+ model, based on the assumption that only pairs with a definite characteristic distance between donors play an important role in the absorption, calls for some supplementation. In particular, it is necessary to consider the compensation limits of applicability of the donor-pair model, and also the question of the influence of neighboring centers on the spectrum of the pair. We present below a qualitative discussion of these questions.

1. Following Shklovskiĭ and Éfros[1], we assume that the impurity potential contains fluctuations of all scales. From these we can separate the large-scale (Gaussian) fluctuations that include a large number of impurities and have a dimension

$$R_c \sim (1-K)^{-1/2} N_d^{-1/3} \gg N_d^{-1/3},$$

as well as small-scale fluctuations, with dimension $R < N_d^{-1/3}$, containing a small number of impurities. The bottom of the conduction band duplicates have variation of the large-scale potential. The change of the energy spectrum of a localized electron is determined primarily by the small-scale fluctuations. The potential wells produced by them contain most electrons as $t \to 0$ (actually, this applies only to the wells inside the large-scale potential well).

Let us see which of the small-scale fluctuations are significant. According to the Poisson distribution, the probability that the volume V (much smaller than the total volume of the system) contains N donors is

$$w(N, V) = \frac{(N_d V)^N}{N!} \exp(-N_d V). \quad (1)$$

The number of clusters of two, three, etc. donors per unit volume (concentration of pairs N_2, "triads" N_3, etc.) is

$$N_2(V) = {}^1/_2 N_d (N_d V)^2 \exp(-N_d V),$$
$$N_3(V) = {}^1/_6 N_d (N_d V)^3 \exp(-N_d V). \quad (2)$$

It is seen from (1) and (2) that the concentration of the clusters of donors producing small-scale potential wells (having a volume $V < \overline{V} = N_d^{-1}$) decreases rapidly with increasing number of donors in the cluster and with decreasing well dimension. The only important clusters, however, are those whose concentration is close to the concentration of the electrons on the donors (n). It is clear, on the other hand, that the more donors participating in the cluster, the deeper will be the potential well produced by them. One can estimate quite roughly at which concentration at $T \to 0$ the pairs are not yet filled and all the electrons are on triads, groups of four, etc. This will be the case if for $V < \overline{V}$ we have

$$N_3(V) > n, \quad (3)$$

i.e., at

$$1-K < 1/6e \approx 0.06, \quad K > 0.94. \quad (4)$$

The numbers in the inequalities (4) are approximate. The purpose of the arguments presented above is to demonstrate that among the small-scale fluctuations the impurity pairs (complexes of the type H_2^+) are significant at concentrations that are bounded not only from below ($K > 0.5$) but also from above. The latter was not taken into account in[1].

2. Assume now that the concentration is such that $N_3(V) \ll n$ at $V < \overline{V}$, and therefore the electrons are

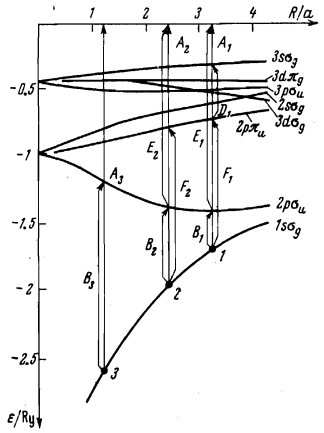

FIG. 7. Energy levels of H_2^+ against the distance between nuclei (in Bohr-radius units). The arrows show the transitions between the H_2^+ levels whose energies are close to the energies of the observed peaks for samples Nos. 1-3.

TABLE II. Oscillator strengths and photoionization cross sections for H_2^+ [16, 17].

Transition	Oscillator strength	Photoionization cross section, 10^{-18} cm^2	R/a
$1s\sigma_g \rightarrow$ "band" (photoionization)		1.29	1
		0.93	2
$\Delta = 0$		1.41	3
$\Delta = 0.22$		0.47	2
$\Delta = 0.45$		0.27	2
$1s\sigma_g \rightarrow 2p\sigma_u$	0.3		1–4
$1s\sigma_g \rightarrow 2p\pi_u$	0.41÷0.45		1–5
$1s\sigma_g \rightarrow 3p\sigma_u$	0.016÷0.004		1–3
$1s\sigma_g \rightarrow 4f\sigma_u$	$4\cdot10^{-4}$		1–3
$1s\sigma_g \rightarrow 4p\sigma_u$	$4\cdot10^{-3}$		1–3
$2p\sigma_u \rightarrow 2s\sigma_g$	0.15÷0.10		1–3
$2p\sigma_u \rightarrow 3d\sigma_g$	0.22÷0.29		1–3
$2p\sigma_u \rightarrow 3s\sigma_g$	10^{-2}		1–3
$2p\sigma_u \rightarrow 3d\pi_g$	0.2÷0.47		0–5
$2p\pi_u \rightarrow 3d\pi_g$	0.25÷0.30		1–3

mainly located on pairs. Then as $T \rightarrow 0$ and at $1-K \ll 1$ all the pairs of the volume $V \leq V_m = 2N_d^{-1}(1-K) \ll V_{av}$ are filled, with the distance between donors $R \leq R_m$ (see (2)). The probability of finding the nearest neighbor of the given donor (which enters in the pair) at a distance R is then proportional to R^2 [14]. Consequently, pairs with $R \approx R_m$ predominate at $V < \overline{V}$.[1)]

Let us discuss qualitatively the influence of the fields of centers close to the pair on its energy spectrum. If the charged centers are randomly distributed, the field exerted on one of them by all the others is determined mainly by the nearest neighbor[14], and the total field of all the remaining centers is small. Consequently, within the limits of the pair, the potential produced by all the remaining centers varies little, i.e., the pair is practically "isolated" from the remaining charged centers. This justifies the consideration of the pair with $R \sim a$ as the analog of an isolated molecular hydrogen ion H_2^+[2].

3. Figure 7 shows the energy levels of H_2^+, constructed from the data of[3], as functions of the distance between nuclei (the Coulomb energy of the nuclear interaction, which is immaterial in what follows, is not taken into account). The curves are marked as follows: 1, 2, 3 ... and s, p, d ... are the principal and orbital quantum numbers of the "unified" nuclei (of the helium atom[15]; σ, π, δ, ... are the projections of the angular momentum on the straight line joining the nuclei, and are equal to 0, ±1, ±2 ... ; the subscripts g and u designate respectively even and odd parity of the coordinate function with respect to inversion at the midpoint of the line joining the nuclei. Table II gives the photoionization cross sections σ_{ph} of the ground state and the oscillator strengths f_{ij} for several fixed distances between the nuclei and for several dipole transitions i → j (see[16] and the references therein).

We note that for R = 2a the photoionization cross section decreases noticeably with increasing $\Delta \equiv (\hbar\omega - \epsilon_{1s\sigma g})/\epsilon_{1s\sigma g}$[17]. (We have no data on $\sigma_{ph}(\Delta)$ for other values of R.) Allowance for the change in the rotational and vibrational levels of H_2^+ in photoionization can greatly increase σ_{ph} (for example, by more than 7 times at R = 2a[16,17]).

For the transition between the localized states with central frequency ω_{ji} and electron concentration in the initial state n_i we can, knowing f_{ij} and assuming the line to have a Lorentz shape, obtain the integral absorption coefficient of the line:

$$K_{ij} = 2\pi^2 \frac{e^2}{m^* c \varkappa^{1/2}} f_{ij} n_i \left[1 - \exp\left(-\frac{\hbar\omega_{ji}}{kT}\right)\right]. \qquad (5)$$

In comparison with[16], the mass of the free electron is replaced here by the effective mass m*, and the dielectric constant of the crystal κ was introduced; the factor in square brackets takes into account the stimulated emission of the photons in the transitions from the state $|j\rangle$ to the state $|i\rangle$.

4. DISCUSSION OF EXPERIMENTAL RESULTS

Let us compare the experimental data with the results of the analysis of the H_2^+ model.

1. The rather close agreement between the energies of the short-wave peaks and the values of ϵ_1 for samples Nos. 1–3 (see Figs. 2–4), and the increase of these energies with increasing K, allows us to suggest that the peaks A_1, A_2, and A_3 are due to photoionization of the ground state of the impurity pair. By identifying the peak energies ϵ_{A_1}, ϵ_{A_2}, and ϵ_{A_3} with the values $\epsilon_{1s\sigma g}$, we can determine the characteristic pair dimensions R_i for samples 1–3. They turn out to be $R_1 \approx 3.3a$, $R_2 \approx 2.5a$, and $R_3 \approx 1.3a$. Since R determines the energy spectrum of H_2^+, we compare, knowing R_i, the energies of the remaining observed peaks (B, C, D, E, F) with the energies of the possible transitions. The arrows in Fig. 7 indicate the allowed transitions that are close in energy to the observed peaks. The difference between the calculated and observed energies of the peaks (B, C, D, E, F) does not exceed 5–7% (cf. Figs. 2–4 and Fig. 7)[2)].

We note that the energies of some peaks (for example, B_1, F_1, F_2) practically coincide with the energies of several different transitions from the ground and excited states with close values of the oscillator strength. Thus, for the peak B_1, the energies of the transitions $1s\sigma_g \rightarrow 2p\sigma_u$, $2p\pi_u \rightarrow 3d\pi_g$ with energies and oscillator strengths $\hbar\omega = 0.30$ Ry, $f \approx 0.27$ and $\hbar\omega = 0.28$ Ry, $f \approx 0.3$, respectively, are close (see Fig. 2 and Table II). It is clear, however, that the transition from the ground state is more intense, in view of its larger population.

The identification of the peaks shows that the strongest transitions in the investigated samples are the following (see Figs. 2–4): 1) photoionization of the ground state; 2) transition from the ground state to the first excited state, $1s\sigma_g \rightarrow 2p\sigma_u$; 3) transition from the ground state to the second excited state, $1s\sigma_g \rightarrow 2p\pi_u$. This is not surprising, since these transitions are the most probable (see Table II). In addition to these transitions, in the least compensated samples No. 1 and No. 2 we observe peaks E_1 and E_2 that can be ascribed to photoionization of the first excited state $2p\sigma_u$, and in sample No. 1 also a peak D

due to transition from the second excited state $2p\pi_u \rightarrow 3s\sigma_g$.

2. The vanishing of the peaks E_1, E_2, and D_1 with decreasing temperature can be attributed to a decrease in the population of the states $2p\sigma_u$ and $2p\pi_u$. If it is assumed that the distribution of the electrons in the impurity band is nondegenerate, then the population of the state $2p\sigma_u$ relative to the ground state is

$$\propto \exp\left[-|\varepsilon_{1s\sigma_g}-\varepsilon_{2p\sigma_u}|/kT\right]$$

and amounts in sample No. 1 to ~0.65 at 4.2°K and ~0.3 at T = 1.6°K, while in sample No. 2 it amounts to ~0.42 and 0.09, respectively, i.e., it decreases quite noticeably with decreasing T. It appears that at 1.6°K the peaks E_1 and E_2 cannot be separated against the background of the stronger photoionization peaks A_1 and A_2. It is possible to explain analogously the vanishing of the peak D_1 at 1.6°K, due to transition from the state $2p\pi_u$, which is separated from the ground state by a gap 0.94 Ry ~7.3°K.

The increase of the intensity of the peaks B_1 and F_1 with decreasing temperature can apparently be attributed to two causes: the increase of the population of the initial state and a certain increase in the factor

$$\beta = 1-\exp(-\hbar\omega/kT)$$

(see (5)). The decrease of the intensities of the peaks A_1 and A_2 at T = 1.6°K in comparison with T = 2.4°K seems therefore strange at first glance. It can probably be explained by assuming that the lowering of the temperature fixes more rigidly the positions of the H_2^+ impurity atoms, and decreases the number of vibrational and rotational levels. This seems to affect little the probabilities of transition between the localized states, but can decrease σ_{ph} (see above). The small shift of the peaks A_1, A_2, B_1, and B_2 towards shorter wavelengths with decreasing temperature can be naturally attributed to the accompanying decrease of pairs with $R > R_m$.

Let us dwell briefly on the change of the peak F_1 with changing temperature. The noticeable increase of its intensity, a certain narrowing, and the shift of 0.1 Ry ~0.8°K towards the shortwave side with decreasing temperature can be explained by assuming that at T = 4.2°K the peak F_1 ($\epsilon_{F_1} \approx 0.76$ Ry) is due to several transitions with nearly equal energies from the ground and excited states (for example, $1s\sigma_g \rightarrow 2p\pi_u$ 0.93 Ry, $2p\sigma_u \rightarrow 2s\sigma_g$–0.8 Ry, $2p\sigma_u \rightarrow 2p\pi_u$–0.66 Ry, photoionization of the states $2p\pi_u$ –0.74 Ry). With decreasing temperature, the intensity of the transitions $2p\sigma_u \rightarrow 2s\sigma_g$, $2p\sigma_u \rightarrow 2p\pi_u$ and of the photoionization of the state $2p\pi_u$ decreases, and that of the transition $1s\sigma_g \rightarrow 2p\pi_u$ increases, so that the latter becomes predominant. A much smaller shift to the shortwave region is experienced by the peak F_2. The apparent cause is that this peak is due to only one transition $1s\sigma_g \rightarrow 2p\pi_u$, and the intensities of the other transitions with close energies, $2p\sigma_u \rightarrow 3d\sigma_g$, $2p\sigma_u \rightarrow 3d\pi_g$, is small because in this sample the excited state $2p\sigma_u$, which is separated from the ground state by 0.56Ry ~5°K, has a small population.

3. Let us now compare the experimentally obtained integral absorption coefficients (K_e) for the peaks B_1 and B_2 at T = 1.6°K with the theoretical value (K_t) expected in accordance with the H_2^+ model (see (5)). We shall assume for estimating purposes that, just as for a Lorentz line, $K_e = \alpha_{abs}(\lambda)\pi\Delta\omega$, where $\alpha_{abs}(\lambda)$ is the absorption coefficient at the maximum of the peak and $\Delta\omega$ is the half-width of the peak. The peak B_1 is asymmetrical, and $\Delta\omega$ will be taken to mean the arithmetic mean of its "narrow" ($\Delta\omega_n \approx 7.2 \times 10^{10}$ sec^{-1}) and "broad" ($\Delta\omega_b \approx 2.2 \times 10^{11}$ sec^{-1}) half-widths (see Fig. 2). This yields $K_e \approx 9 \times 10^{12}$ cm^{-1} sec^{-1}. For sample No. 1, according to (5), we obtain $K_t \approx 1.3 \times 10^{13}$ cm^{-1} sec^{-1}, which is only 1.5 times the experimental value. For the peak B_2, the ratio of the calculated and experimental values is approximately the same.

A much greater discrepancy between theoretical ($\alpha_t(\lambda) = n\sigma_{ph}^{abs}$) and experimental ($\alpha_e(\lambda)$) values of the absorption coefficient is observed for the photoionization peaks of the ground state (A). (Here $\sigma_{ph}^{abs} = (a/a_0)^2 \kappa^{-1/2}$ is the photoionization cross section of a molecular ion "placed" in a semiconductor, a_0 is the Bohr radius of the electron in free space). Thus, for example, if we use the values of σ_{ph} at fixed R, then we get for sample No. 3 (at $\Delta = 0$) the value $\alpha_t \approx 3$ cm^{-1} for a $\approx 6.4 \times 10^{-6}$ cm and $\kappa \approx 16$. The experimental value α_e for sample No. 3 turned out to be ~20 cm^{-1} (Fig. 4). So large an excess of the experimental value of $\alpha_e(\lambda)$ over the calculated value is also observed for samples Nos. 1 and 2. It cannot be attributed to possible measurement errors. It is possible, however, that this difference, as well as the decrease of the intensities of the peaks A_1 and A_2 with decreasing temperature, indicates that the impurity pair in the crystal is not "rigid" and that it is necessary to take into account the change of the vibrational levels on photoionization, which greatly increases σ_{ph}. Thus, the good agreement between K_t and K_e and the appreciable excess of α_e over α_t, as well as the change of the intensities of the peaks with changing temperature (see above) all indicate that the thermal lattice vibrations are much more important for the photoionization of the impurity pair (H_2^+) than for the transitions between the localized states.

4. Let us discuss the influence of "band-band" illumination on the form of $\alpha(\lambda)$. The results shown in Fig. 6 for sample No. 3 can apparently be explained in the following manner. Illumination greatly increased the concentration of the electrons in the impurity band, which is equivalent to decreasing the compensation. This has led to the filling of the donor pairs with larger distances between donors than before, and increased the characteristic dimension R_3 of the pair. If, as before, we ascribe the short-wave peak A_3' (Fig. 3) to photoionization of the ground state, then $R_3' \approx 2.3a$ (we recall that the characteristic distance for the peak A_3 is $R_3 \approx 1.3a$). The value of R_3' is, of course, somewhat arbitrary, since the peak A_3' is quite broad. Then the peaks 1.5 Ry and 1.15 Ry can be attributed to the transitions $1s\sigma_g \rightarrow 3p\sigma_u$, $3d\pi_g$ ($\Delta\epsilon \sim 1.6-1.56$ Ry) and to the transition $1s\sigma_g \rightarrow 2p\pi_u(F_3')$ (1.24 Ry). The peak $1s\sigma_g \rightarrow 2p\sigma_u$ observed without the additional illumination can have at $R_3' \sim 2.3a$ an energy ~0.7 Ry, which is outside the range of observable frequencies.

5. We note that in none of the samples did we observe peaks that could be ascribed with certainty to the hydrogen-like spectrum of the isolated donor D^0. The absence of hydrogenlike absorption lines can apparently be attributed only to the small number of filled donors D^0. This agrees with the experimentally observed activation energy $\epsilon_1 > 1$ Ry (see Table I).

6. We proceed now to discuss the experimental data on $\alpha(\lambda)$ in samples 4–6. We note first that qualitatively similar $\alpha(\lambda)$ dependences were obtained earlier[13] for compensated n-InSb samples with strong and intermediate doping ($N_d a^3 \gtrsim 1$). These results were attributed by

Gal'pern and Éfros[18] to absorption by almost free electrons situated in large-scale potential wells or metallic drops that were isolated from one another. However, samples 4–6 were known to be weakly doped, $N_d a^3 \lesssim 4 \times 10^{-2}$ and $N_d^{-1/3} \sim 3a$, and the theory of[18] does not apply to them. On the other hand, as noted above, the H_2^+ model also becomes invalid with increasing compensation. Therefore the fact that samples 4–6 do not possess the absorption spectrum typical of H_2^+ is not surprising. Moreover, from the fact that the $\rho(T)$ curves (see Fig. 1) have no sections with activation energies $\epsilon_1 \lesssim 4$ Ry ~ 2.7 meV it also follows that in samples 4–6 the wells made up by the donor pair are apparently negligible.

It is natural to use two alternative models to explain the absorption in samples 4–6: 1) the model of triads with one electron, and 2) the model of the disordered semiconductor. For the disordered semiconductor, however, the absorption has been considered theoretically only in the low-frequency region (see, e.g.,[6]), and even in this case the results obtained by different workers did not agree[6]. The energy levels and the wave functions for a system of three charged centers are not known. It is clear, however, that in the case of triads the absorption spectrum can be more smeared out than for impurity pairs (H_2^+). Indeed, the energy spectrum of the pair is determined by one quantity, R, and pairs with $R \sim R_m$ predominate, while the spectrum of a triad is determined by three quantities, namely the distance from a given donor to the first ($|\mathbf{r}_1|$) and to the second ($|\mathbf{r}_2|$) nearest neighbors, and by the angle between $\mathbf{r}_1$ and $\mathbf{r}_2$. In addition, a pair can be regarded as almost "isolated" (see above). This is hardly true for the triad. We therefore believe it possible that the absorption spectrum in samples 4–6 is due to a transition of the electrons from the band of the ground states of the triads to the smeared band of the excited states.

The foregoing discussion shows that with the aid of the model of the molecular ion H_2^+ it becomes possible to explain satisfactorily the majority of experimental facts – the positions of the peaks, the dependence of their intensities on the temperature, the absolute values of the integral absorption coefficient – for the least compensated n-InSb samples. Consequently, the energy spectrum of the localized electrons in these samples is analogous to the spectrum of the molecular hydrogen ion H_2^+ with $R \sim (1-3.5)a$. In more compensated samples, the energy spectrum is significantly different. The form of this spectrum is still an open question.

The authors are deeply grateful to Yu. A. Gurvich for a discussion of the results and to S. R. Filonovich for help with the experiment.

[1)] Actually, pairs with $R > R_m$ are also filled at $T > 0$, but their number is small because of the rapid decrease of the filling probability with increasing R.

[2)] In sample No. 1, the energy of the short-wave peak at T = 1.6°K amounts to 1.58Ry ($R \approx 3.6a$). We have chosen, however, $R \approx 3.3a$ ($\epsilon_{1s\sigma_g} = 1.68$Ry), which gives better agreement with the experiment for the remaining peaks observed in the sample.

[1] B. I. Shklovskiĭ and A. L. Éfros, Materialy chetvertoĭ zimneĭ shkoly po fizike poluprovodnikov (Materials on the fourth Winter School on the Physics of Semiconductors), Physico-technical Institute, Leningrad, pp. 552-577, 1972; Zh. Eksp. Teor. Fiz. **60**, 867 (1971) [Sov. Phys.-JETP **33**, 468 (1971)]; B. I. Shklovskiĭ, Fiz. Tekh. Poluprov. 7, 1197 (1972) [Sov. Phys.-Semicond. **7**, 803 (1972)].
[2] V. V. Arendarchuk, E. M. Gershenzon, L. B. Litvak-Gorskaya, and R. I. Rabinovich, ZhETF Pis. Red. **17**, 237 (1973) [JETP Lett. **17**, 169 (1973)].
[3] J. Slater, Electronic Structure of Molecules, McGraw-Hill, 1963. D. R. Bates, K. Ledsham, A. L. Stewart. Phil. Trans. Roy. Soc. (London), **246**, 215, 1953.
[4] J. Blinowski and I. Mycielski, Phys. Rev. **136**, A266 (1965); **140**, A1024 (1965).
[5] M. Pollak and T. H. Geballe, Phys. Rev. **122**, 1742 (1961); N. Nagakawa, H. Yoshinaga. J. Phys. Soc. Japan, **30**, 1212, 1971. A. I. Demeshina, R. L. Korchazhkina, N. N. Kuznetsova, and V. N. Murzin, Fiz. Tekh. Poluprov. 4, 428 (1970) [Sov. Phys.-Semicond. 4, 363 (1970)].
[6] N. F. Mott, Electrons in Disordered Structures, Russ. Transl., Mir, 1969. V. L. Bonch-Bruevich, Zh. Eksp. Teor. Fiz. **59**, 985 (1970) [**32**, 536 (1971)].
[7] E. M. Gershenzon, V. S. Ivleva, I. N. Kurilenko, and L. B. Litvak-Gorskaya, Fiz. Tekh. Poluprov. **6**, 1982 (1972) [Sov. Phys-Semicond. **6**, 1695 (1973)]; E. M. Gershenzon, I. N. Kurilenko, and L. B. Litvak-Gorskaya, ibid. **6**, 2401 (1972) [**6**, 2011 (1973)].
[8] V. V. Arendarchuk, E. M. Gershenzon, and L. B. Litvak-Gorskaya, ibid. 7, 132 (1973) [**7**, 89 (1973)].
[9] A. N. Vystavkin and L. K. Mel'nik, Prib. Tekhn. Éksperim. No. 1, 189 (1963).
[10] M. B. Golant, R. L. Vilenskaya, E. A. Zyulina, Z. F. Kaplun, A. A. Negirev, V. A. Parilov, G. B. Rebrov, and V. S. Savel'ev, ibid., No. 4, 136 (1965).
[11] E. M. Gershenzon, V. A. Il'in, and L. B. Litvak-Gorskaya, Fiz. Tekh. Poluprov. 8 (1973) [Sov. Phys.-Semicond. 8 (1973)].
[12] V. F. Bannaya, E. M. Gershenzon, and L. B. Litvak-Gorskaya, ibid. **2**, 978 (1968) [**2**, 812 (1969)].
[13] A. N. Vystavkin, Yu. S. Gal'pern, and V. N. Gubankov, ibid. **1**, 1735 (1967); **2**, 1651 (1968) [**1**, 1439 (1967); **2**, 1373 (1969)].
[14] I. I. Sobel'man, Vedenie v teoriyu atomnykh spektrov (Introduction to the Theory of Atomic Spectra), Fizmatgiz, 1963.
[15] G. Herzberg, Molecular Spectra and Molecular Structure, Vol. 1, Van Nostrand, 1950.
[16] R. Nichols and A. Stewart, in: Atomic and Molecular Processes (D. R. Bates, ed.). Acad. Press, 1962.
[17] D. R. Bates, U. Opic, and G. Poots, Proc. Phys. Soc. **A66**, 1113 (1953).
[18] Yu. S. Gal'pern and A. L. Éfros, Fiz. Tekh. Poluprov. **6**, 1081 (1972) [Sov. Phys.-Semicond. **6**, 941 (1972)].

Translated by J. G. Adashko
249